STATE UNIVERSITY OF NEW YORK
AT STONY BROOK

COLLEGE OF
ENGINEERING

Report No. 100

BEHAVIOR OF SPHERICAL SOLID PARTICLES RELEASED IN A LAMINAR BOUNDARY LAYER ALONG A FLAT PLATE

by

Shao-lin Lee and Elizabeth B. Dussan

November, 1967

BEHAVIOR OF SPHERICAL SOLID PARTICLES RELEASED IN A LAMINAR BOUNDARY LAYER ALONG A FLAT PLATE

By

Shao-lin Lee
Associate Professor

and

Elizabeth B. Dussan V.
Research Assistant

Department of Mechanics
State University of New York At Stony Brook

Report No. 100

November, 1967

SUMMARY

This is a study of a very small particle leaving the surface of a flat plate and entering a surrounding laminar boundary layer. The Stokes drag in the horizontal and vertical directions is the only force acting on the particle. As a consequence of the above two statements the fluid Reynolds number is $R_E \gg 1$ and the particle Reynolds number is $R_e \ll 1$. The governing equations are two simultaneous, second order, ordinary, nonlinear differential equations with one parameter. A complete digital computer solution and analytic limiting solution for large and small values of the independent variable, T, have been obtained. Both numerical and analytic solutions are in close agreement. Results are presented in the form of the trajectory of the particle, and also the forces acting on the particle and the absolute velocity of the particle at every point in the trajectory. It has been found that the particle comes into equilibrium with the fluid very quickly with respect to the spatial coordinates, raising only several radii from the surface in its entire flight.

NOTATION

$R_E = \frac{u_\infty \mathrm{X}}{\nu}$

$R_e = \frac{|\underset{\sim}{V}_g - \underset{\sim}{V}|\, d}{\nu}$

R = radius

$\underset{\sim}{V}$ = velocity of particle

t = time

ρ = density

$\underset{\sim}{F}$ = force

$\underset{\sim}{\Omega}$ = angular vel. of particle

u = velocity of fluid in horizontal direction

X = dimensional horizontal distance from the leading edge

$X = \frac{\mathrm{X}}{\mathrm{X}_o}$ dimensionless horizontal distance from the leading edge

$\mathrm{X}_o = \mathrm{X}|_{t=0}$

$T = \frac{18 \rho_f u_\infty^2 t}{\nu \rho_s R_{ep}^2}$ dimensionless time

$R_{ep} = \frac{u_\infty d}{\nu}$

$\overline{u_g} = u_\infty \beta \mathrm{Y} \sqrt{\frac{u_\infty}{\nu \mathrm{X}}}$

$u_g = \frac{\overline{u_g}\, \nu}{\mathrm{X}_o u_\infty^2}$

$\lambda = \frac{18 \rho_f}{\rho_s R_{ep}^2}$

Y = dimensional vertical distance from plate

$Y = \frac{\mathrm{Y}}{d}$

d = 2 R

β = .332

$\overline{v_g} = \frac{\beta}{4} \sqrt{\frac{\nu u_\infty}{\mathrm{X}}}\ \frac{\mathrm{Y}^2 u_\infty}{\nu \mathrm{X}}$

sub script

g, f	fluid
p, s	particle
L	left
m	Magnus

$$v_g = \frac{\overline{v_g}\ \nu}{d\ u_\infty^2}$$

$$\gamma = \frac{Re_p}{Re_{X_0}^{3/2}}$$

$$Re_{X_0} = \frac{u_\infty X_0}{\nu}$$

$$\alpha = \frac{\gamma}{\lambda}$$

δ = boundary layer thickness

F_s = Stokes drag force.

INTRODUCTION

The effects of rotation, shape, and acceleration of the particle; the shear, inertia and non-Newtonian properties of the fluid; and the presence of a rigid wall and gravity have been neglected.

F. P. Bretherton [3] investigated the motion of particles of different shapes in Couette flow and concluded that this does not affect the trajectory of "very" small particles.

F. Odar and W. S. Hamilton [4] experimentally oscillated a particle in a still fluid such that the particle attained large accelerations and small velocities. Their results agreed with the Basset-Boussinesq-Oseen equation:

$$-\underset{\sim}{F} = 6\pi R\mu \underset{\sim}{V} + \frac{1}{2}\left(\frac{4}{3}\pi R^3\right)\rho_f \dot{\underset{\sim}{V}} + 6R^2(\pi\mu\rho_f)^{1/2}\int_0^t \frac{\dot{\underset{\sim}{V}}(t')}{(t-t')^{1/2}}\,dt'$$

where the first term is the same as the Stokes drag, and the second term is the same as the virtual mass effect in a perfect fluid.

S. T. Rubinow and J. B. Keller [5] investigated, theoretically, a spinning particle with $R_e < 1$. They found that the angular velocity does not affect the Stokes drag; and that the particle experiences a vertical force, $\underset{\sim}{F_L}$, orthogonal to its direction of motion:

$$\underset{\sim}{F_L} = \pi R^3 \rho_s \underset{\sim}{\Omega} \times (\underset{\sim}{V_g} - \underset{\sim}{V}) \tag{1}$$

this force is used to explain the curving of a pitched baseball and the long range of a spinning golf ball. These are examples of particles initially having a rotation.

R. B. Edelman and D. H. Kiely [1] investigated the flow of a dilute suspension of solids in a laminar gas boundary layer. The force in the vertical direction considered in the study is:

$$\underset{\sim}{F_m} = \frac{4}{3}\pi R^3 \rho_f (\underset{\sim}{V_f} - \underset{\sim}{V}) \frac{d u_f}{dY} \tag{2}$$

this is called the Magnus force. The force is produced by the velocity difference between the upper and lower portion of the particle caused by the shear in the velocity field.

GOVERNING EQUATIONS

The equations of motion in dimensionless form of the particle, undergoing a Stokes drag in the horizontal and vertical directions, with stretched time variable are:

$$\frac{d^2X}{dT^2} = u_g \alpha - \frac{dX}{dT} \tag{1-a}$$

$$\frac{d^2Y}{dT^2} = v_g \alpha - \frac{dY}{dT} \tag{1-b}$$

where

$$\alpha = \frac{\rho_s Re_p^3}{18 \rho_f Re_{X_0}^{3/2}}, \qquad T = \frac{18 \rho_f u_\infty^2 t}{\nu \rho_s Re_p^2},$$

$X = \frac{\mathrm{X}}{\mathrm{X}_0}$, $Y = \frac{\mathrm{Y}}{d}$, u_g and v_g are components of the gas velocity in the horizontal and vertical direction in dimensionless form respectively. It is assumed that $\eta = \mathrm{Y}\sqrt{\frac{u_\infty}{\nu \mathrm{X}}} \ll 1$ at $T = 0$, implying that the dimensions of the particle are small compared with the boundary layer thickness at X_0 $(d \ll \delta)$, this is a necessary condition for a particle to be considered small. Therefore, it is valid to use initially only the first term in the Blasius series solution for the velocity profile in the laminar boundary layer.

$$v_g = \frac{\nu}{d u_\infty^2}\left(\frac{\beta \mathrm{Y}^2 u_\infty}{4 \nu \mathrm{X}} \sqrt{\frac{\nu u_\infty}{\mathrm{X}}}\right) \tag{2-a}$$

$$u_g = \frac{\nu}{X_o u_\infty^2}\left(\beta u_\infty Y \sqrt{\frac{u_\infty}{\nu X}}\right) \tag{2-b}$$

It is shown in the results that for realistic values of α the first term in the Blasius series solution is sufficient for all time. The governing equations with the above assumptions are:

$$\frac{d^2X}{dT^2} = \alpha\beta\frac{Y}{X^{1/2}} - \frac{dX}{dT} \tag{3-a}$$

$$\frac{d^2Y}{dT^2} = \frac{\beta Y^2}{4X^{3/2}} - \frac{dY}{dT} \tag{3-b}$$

METHOD OF SOLUTION

An analytic small time series solution has been obtained by expanding the dependent variables X and Y in terms of the independent variable T,

$$Y = A_o + A_1 T + \cdots + A_5 T^5 + \cdots \tag{4-a}$$

$$X^{1/2} = B_o + B_1 T + \cdots + B_5 T^5 + \cdots \tag{4-b}$$

substituting into Eq's. (3-a) and (3-b), and equating the coefficients of like powers of T. The first two coefficients in each series are determined by the initial conditions

$$\left.\begin{matrix}\dfrac{dX}{dT} = \dfrac{dY}{dT} = 0 \\ X = 1, \quad Y = \frac{1}{2}\end{matrix}\right\} \quad \text{at } T = 0 \tag{5}$$

resulting in

$$A_o = \tfrac{1}{2}, \qquad A_1 = 0$$
$$B_o = 1, \qquad B_1 = 0$$

The other coefficients are:

$$A_2 = \frac{\alpha\beta}{32}\ ; \quad A_3 = -\frac{\alpha\beta}{24}\ ; \quad A_4 = \frac{\alpha\beta}{384}\left(1 - \tfrac{1}{2}\alpha\beta\right); \quad A_5 = \frac{\alpha\beta}{1920}(\alpha\beta - 1); \cdots$$

and

$$B_2 = \frac{\alpha\beta}{8}\;;\quad B_3 = -\frac{\alpha\beta}{24}\;;\quad B_4 = \frac{\alpha\beta}{96}\left(1-\frac{7}{8}\alpha\beta\right)\;;\quad B_5 = \frac{\alpha\beta}{96}\left(\frac{7}{40}\alpha^2\beta^2+\frac{3}{8}\alpha\beta-\frac{1}{5}\right), \ldots$$

At large time the solid particle is in equilibrium with the surrounding fluid. The governing equations of motion reduce to:

$$\frac{dY}{dT} = v_g = \frac{\alpha\beta Y^2}{4X^{3/2}} \tag{6-a}$$

$$\frac{dX}{dT} = u_g = \frac{\alpha\beta Y}{X^{1/2}} \tag{6-b}$$

With the exact analytic solutions being:

$$Y = \left(\tfrac{1}{2}\right)^{6/5}\left[\tfrac{5}{4}\alpha\beta T + 2\right]^{1/5} \tag{7-a}$$

$$Y = \tfrac{1}{2}X^{1/4} \tag{7-b}$$

Equations (3-a) and (3-b) have also been solved numerically using the predictor-corrector method [2]. This method needs two preceding points, say R_m and R_{m-1}, to predict the next point R_{m+1} (R_m is the dependent variable).

$$R_{m+1} = R_{m-1} + 2h\,f(R_m, S_m)$$

and correct by

$$R_{m+1}^{(i)} = R_m + \frac{h}{2}\left[f(R_m, S_m) + f\left(R_{m+1}^{(i-1)}, S_{m+1}\right)\right]$$

the superscripts correspond to the number of times the point, R_{m+1}, has been corrected (predict = superscript (o)), and h corresponds to the increment in the independent variable S, where

$$\frac{dR}{dS} = f(R, S)$$

The correcting process stops when $\left|R_{m+1}^{(i)} - R_{m+1}^{(i-1)}\right| < \epsilon$

where $\epsilon > 0$

Equations (3-a) and (3-b) can be expressed as four simultaneous ordinary differential equations with four dependent variables

$$\frac{dX}{dT} = u , \qquad \frac{du}{dT} = \alpha u_g - u$$

$$\frac{dY}{dT} = v , \qquad \frac{dv}{dT} = \alpha v_g - v$$

The above equations are of a form that can be solved by the predictor-corrector method.

ERROR ANALYSIS

Three methods of error analysis were used to check and correct the error in the computer (numerical) solution.

The first method consisted of reducing the size of the intervals of integration. The intervals were contracted until the small time results were invariant to any further reduction of size. This produced excellent agreement with the analytic small time solution. This is an important point because large error is normally acquired by the computer when there are large gradients. In this problem the largest gradients occur at very small time.

The second method consisted of computing numerically in each time interval E_{X1} and E_{Y1} :

$$E_{X1} = \left| \frac{\frac{u_m - u_{m-1}}{\Delta T} - [\alpha u_{g_m} - u_m]}{\alpha u_{g_m} - u_m} \right|$$

$$E_{Y1} = \left| \frac{\frac{v_m - v_{m-1}}{\Delta T} - [\alpha v_{g_m} - v_m]}{\alpha v_{g_m} - v_m} \right|$$

where $\frac{v_m - v_{m-1}}{\Delta T}$ is the local acceleration of the particle at time

$T = m\Delta T$ (m being a positive integer). The numbers calculated for E_{Y1} and E_{X1} acquire meaning by comparing their value for small and large time. At small time, it is already known that the computer results are good. If the values of E_{Y1} and E_{X1} for large time remain of the same order as they were for small time, this will give some confidence in the results for large time.

The third method consists of evaluating numerically an integrated form of the basic equations

$$u_{2m} \triangleq \int_0^{m\Delta T} \left[\alpha u_g(\tau) - u(\tau)\right] d\tau$$

$$v_{2m} \triangleq \int_0^{m\Delta T} \left[\alpha v_g(\tau) - v(\tau)\right] d\tau$$

and calculating E_{X2} and E_{Y2} .

$$E_{X2} = \frac{u_{2m} - u_m}{u_m}$$

$$E_{Y2} = \frac{v_{2m} - v_m}{v_m}$$

At every point $T = m\Delta T$ the terms v_g , v , u_g , u are known from the solution of the problems. Therefore v_{2m} and u_{2m} can be easily calculated (from existing results). E_{X2} and E_{Y2} are interpreted in the same manner as E_{X1} and E_{Y1} .

RESULTS

Four basic terms appear in equations (3-a) and (3-b). They are $\frac{\rho_f}{\rho_s}$, $R_{ep} = \frac{u_\infty d}{\nu}$, $R_{eX_0} = \frac{u_\infty X_0}{\nu}$ and $\frac{u_\infty^2}{\nu}$. The parameter, α , consists of two parts $\alpha = \frac{\gamma}{\lambda}$. The first term, γ , is dependent of the initial position, $\gamma = \frac{R_{ep}}{R_{eX_0}^{3/2}}$, and the second term, λ , contains the properties of the fluid and the solid, $\lambda = \frac{18\rho_f}{\rho_s R_{ep}^2}$. A large value of α

corresponds to a large particle located close to the leading edge within a fluid such that $\frac{\rho_s}{\rho_f} >> 1$. A realistic upper limit is $\alpha = 1$.

Graphs (see Figs. 1, 2, 3 and 4) contain the results of the computer calculations. Let us examine the curves for $\alpha = 1$. Fig. 1 shows the particle initially at zero velocity at X = 1. The particle reaches very quickly a maximum velocity as it moves down the plate from the leading edge, and then falls off slowly to zero again. The values for the velocities u and v have the same characteristics but in all cases the maximum value of the velocity u is reached after that of the velocity v. It should be noted that the values of the ordinate in curve (2A), v for $\alpha = 1$, must be multiplied by one thousandth to obtain its actual value. Therefore, the maximum value for the velocity v for $\alpha = 1$ is 0.0166.

Fig. 2 shows the force acting on the particle at given distances from the leading edge. Initially there is a positive force corresponding to the surrounding fluid traveling faster than the solid particle. When the particle reaches its maximum velocity in Fig. 1, Fig. 2 shows zero force; that is to say, the surrounding fluid and the solid particle are traveling at the same speed. The particle then advances into slower moving fluid and there is a negative force acting on the particle, or, the slower fluid is trying to hold back the particle. Even though the particle is now going faster than the surrounding fluid, the solid particle is itself slowing down, as it can be seen in Fig. 1. The solid particle reaches a maximum negative difference in velocity with the fluid and then tends (in all cases of α) assymptotically to the same velocity as the fluid. This occurs for both vertical and horizontal directions at different times.

Fig. 3 shows the trajectory of the solid particle. The solid particle which follows the $\alpha = .1$ curve comes into equilibrium with the fluid very quickly with respect to the spatial variables. Coincidentally, the trajectory for $\alpha = .1$ is the same as that for a fluid particle which, at one time, occupied the point $Y = 1/2$, $X = 1$. The solid line (2) represents the trajectory of a solid particle with $\alpha = 1$. At $X \cong 3.66$ the solid particle comes into equilibrium with the fluid. The dashed line which meets the solid line at this point, line (2A), represents the trajectory of the fluid particle, or the stream line, which the solid particle comes into equilibrium. In other words, the dashed line, (2A), represents the stream line that a solid particle's trajectory, with $\alpha = 1$, eventually coincides. The computer solutions for $\alpha = 10$ and $\alpha = 100$ were not carried out to the time of equilibrium with the fluid. The stream lines that they coincide with when they are at equilibrium with the fluid are not known due to the growth in error in the computer solution.

Since solid particles for $\alpha = 0.1$ and $\alpha = 1$ are in equilibrium with the fluid at $X = 5$, the trajectory of the solid particles for $X>5$ is the same as the corresponding stream line and, therefore, can be calculated by equation (7-b).

It is assumed throughout this study that $\eta < 1$ for the solid particle and that equation (2-a) and (2-b) are applicable at all times. Firstly, if $\alpha < .1$ the largest value of η for the particle is its initial value. For solid particles of $\alpha < .1$, the trajectory is the same as the stream line which passes through $Y = 1/2$, $X = 1$. Initially $\eta\Big|_{T=0} = \left[\dfrac{Re_p\, Y}{Re_{X_o}^{1/2} X^{1/2}}\right]\Bigg|_{T=0}$ is assumed $\eta\Big|_{T=0} = \dfrac{Re_p}{2Re_{X_o}^{1/2}} < 1$, which was justified at the beginning of the paper. Rewriting $\eta = \dfrac{Re_p}{2Re_{X_o}^{1/2} X^{1/4}}$ as time increases $T>0$, $X>1$ therefore

$\eta < \eta \big|_{T=0} < 1$. Secondly, it is easily seen that this is true for $\alpha = 1$, and it should be kept in mind that $\alpha = 1$ is the realistic upper limit.

In light of the results presented the Magnus force, lift force due to the rotation of the fluid, and the Stokes drag in the vertical direction may be compared for their relative significance. If we let Ω equal the local angular rotation of the fluid, we find the lift force due to rotation of the particle, F_L, and the Magnus force, F_m, to differ by a factor of 8/3. Next, let us consider F_L/F_S:

With
$$u_g - u = u_g \big|_{T=0}$$
$$v_g - v = v_g \big|_{T=0}$$

Then
$$\frac{F_L}{F_S} = \frac{\beta}{3} \, Re_p \, Re_{x_o}^{1/2}$$

The Stokes drag is larger than the lift force only for extremely small particles.

These results indicate that the same problem with many particles initially at different positions on the plate must also consider the possibility of interaction (collision).

It is also evident that it would be difficult to obtain good experimental data of the trajectory of "extremely" small particles for the purpose of determining the velocity profile of the laminar boundary layer due to the very low flight of the particle. Irregularities in the plate of the same order of magnitude as the diameter of the particle will most probably cause the particle to follow a different trajectory than that predicted in this study.

ACKNOWLEDGMENT

The authors wish to express their sincerest appreciation to the National Science Foundation for its generous support which has made this investigation possible.

BIBLIOGRAPHY

1. - R. B. Edelman and D. H. Kiely, "The Flow of a Dilute Suspension of Solids in a Laminar Gas Boundary Layer", U. S. Naval Ordnance Lab., Oak Ridge, Md., 1964.

2. - W. S. Dorn and D. D. McCracken, "Numerical Methods and Fortran Programming", J. Wiley & Sons, N. Y. 1964.

3. - F. P. Bretherton, "The Motion of Rigid Particles in a Shear Flow at Low Reynolds Number", J. of Fluid Mechanics, v. 14, p. 284, 1962.

4. - Odar, Fuat & Hamilton, Wallis S., "Forces on a Sphere Accelerating in a Viscous Fluid, J. of Fluid Mechanics, v. 18, p. 302, 1964.

5. - Rubinow, S. I. & Keller, Joseph B., "The Transverse Force on a Spinning Sphere moving in a Viscous Fluid", J. of Fluid Mechanics, v. 11, p. 447, 1961.

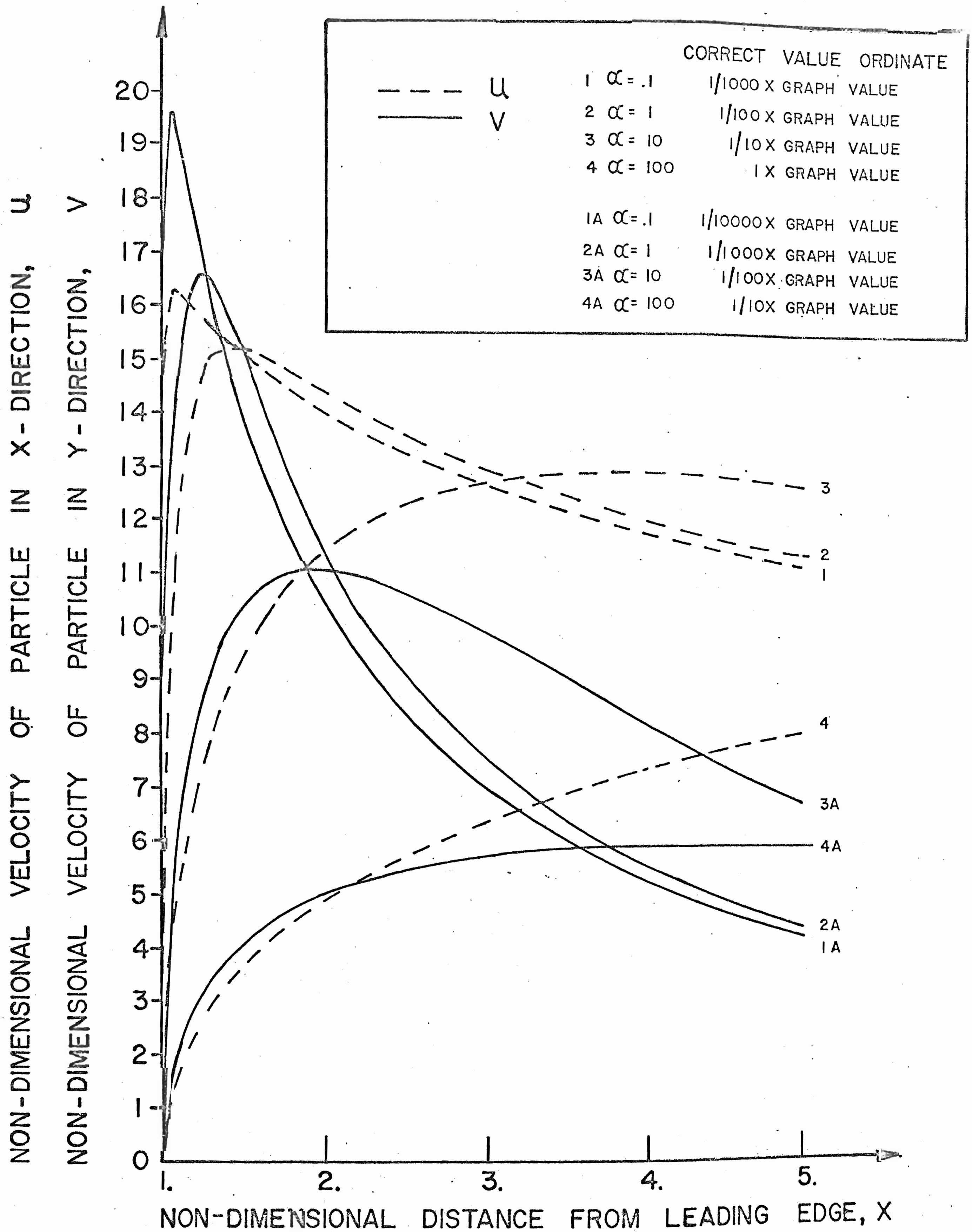

Figure 1, COMPONENTS OF VELOCITY OF PARTICLE

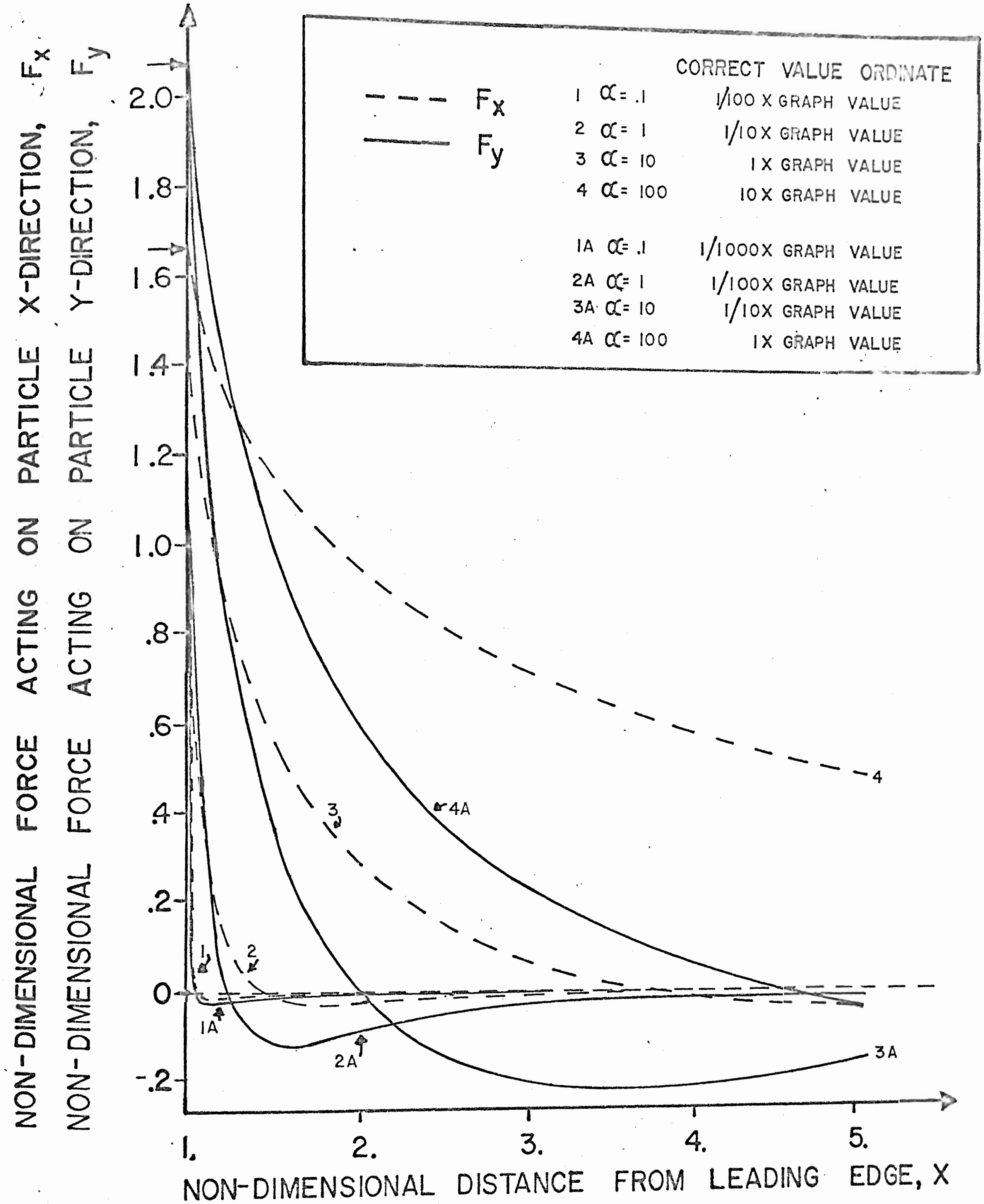

Figure 2, COMPONENTS OF FORCE ACTING ON PARTICLE

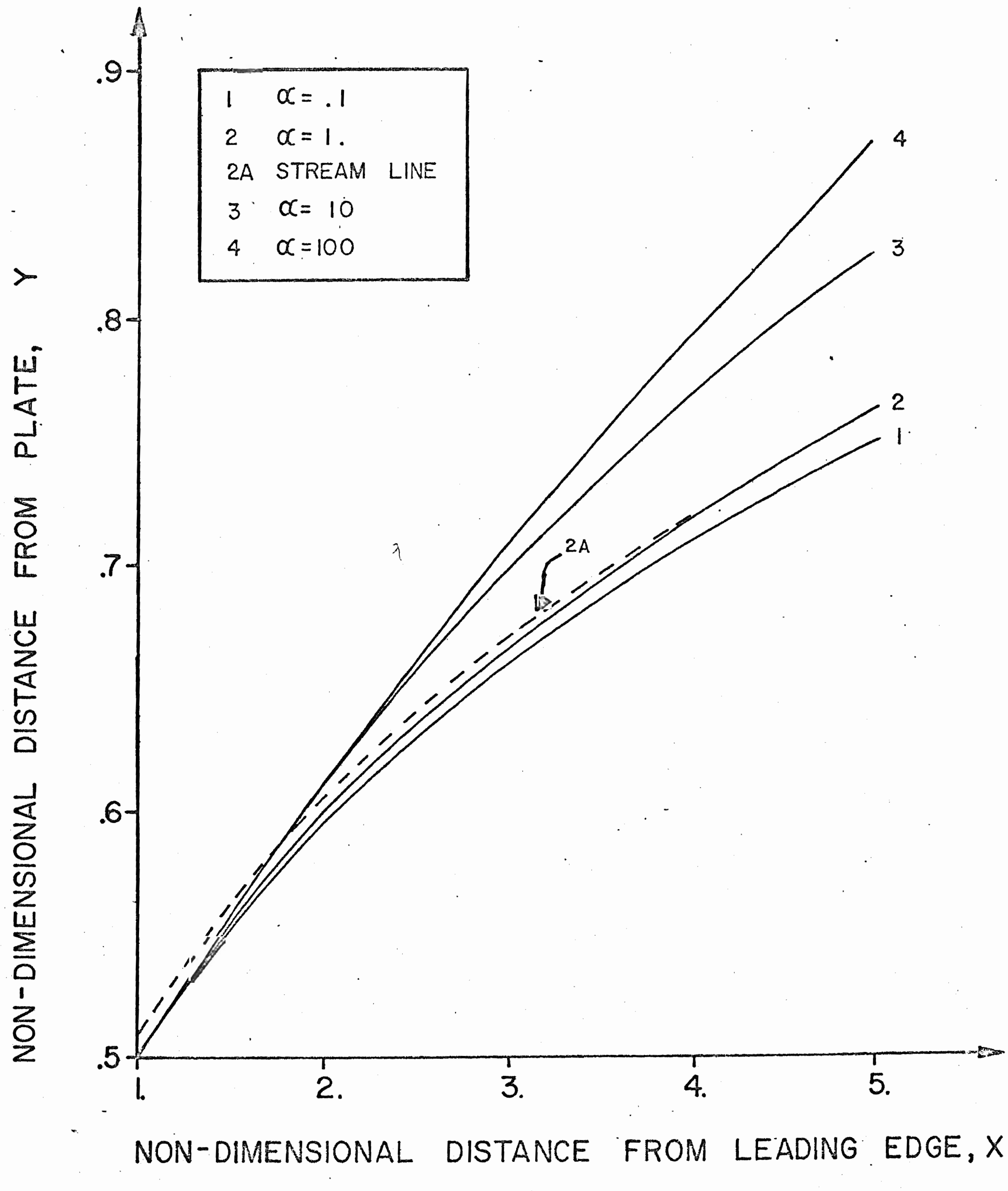

Figure 3, PARTICLE TRAJECTORIES

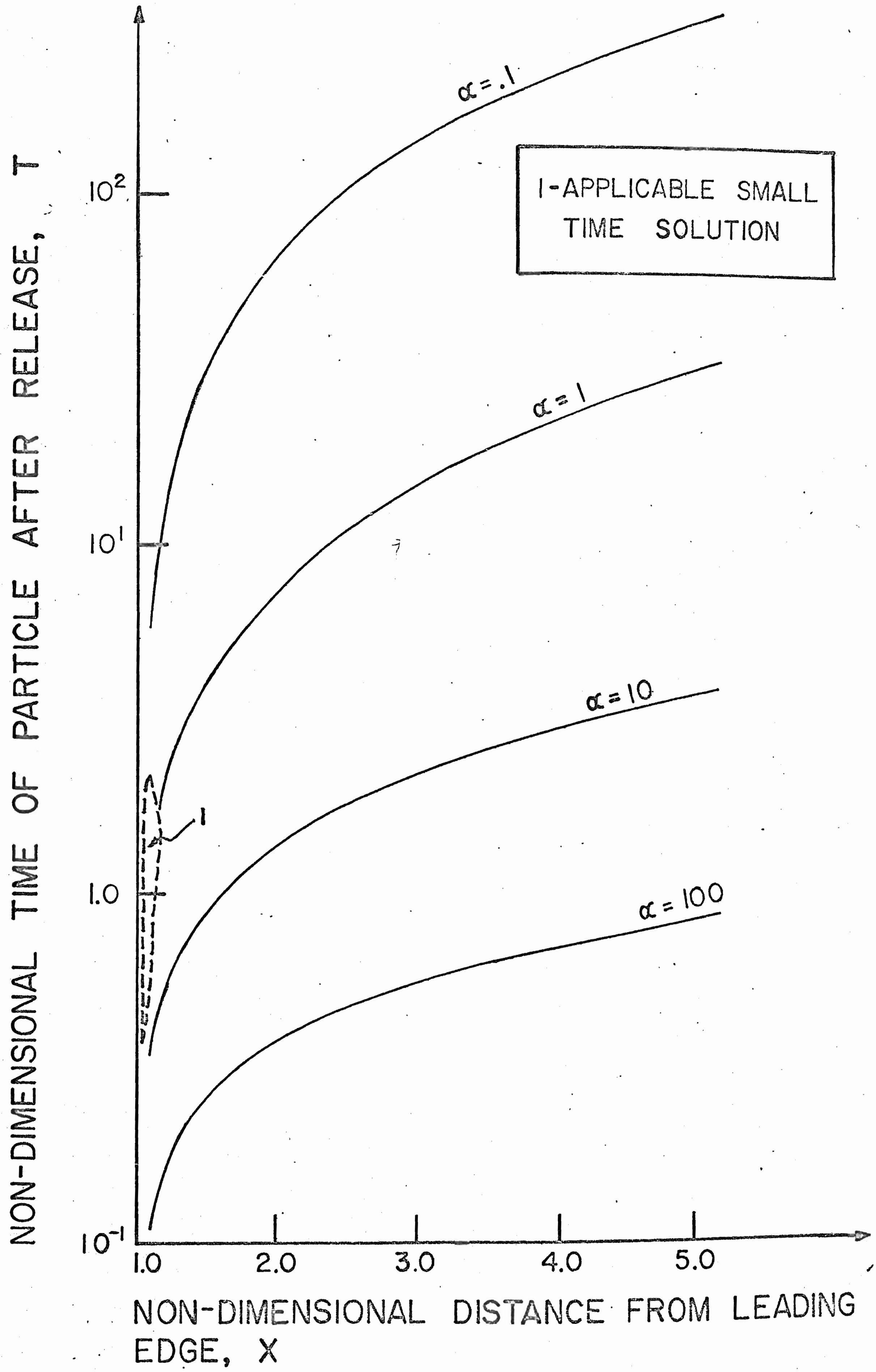

Figure 4, TIME HISTORY OF PARTICLE